

G.F. Matthews, the ASDEX-Upgrade Team  
and JET EFDA contributors

# Plasma Operation with Metallic Walls: Direct Comparisons with the All Carbon Environment

“This document is intended for publication in the open literature. It is made available on the understanding that it may not be further circulated and extracts or references may not be published prior to publication of the original when applicable, or without the consent of the Publications Officer, EFDA, Culham Science Centre, Abingdon, Oxon, OX14 3DB, UK.”

“Enquiries about Copyright and reproduction should be addressed to the Publications Officer, EFDA, Culham Science Centre, Abingdon, Oxon, OX14 3DB, UK.”

The contents of this preprint and all other JET EFDA Preprints and Conference Papers are available to view online free at [www.iop.org/Jet](http://www.iop.org/Jet). This site has full search facilities and e-mail alert options. The diagrams contained within the PDFs on this site are hyperlinked from the year 1996 onwards.

# Plasma Operation with Metallic Walls: Direct Comparisons with the All Carbon Environment

G.F. Matthews<sup>1</sup>, the ASDEX-Upgrade Team<sup>2</sup>  
and JET EFDA contributors\*

*JET-EFDA, Culham Science Centre, OX14 3DB, Abingdon, UK*

<sup>1</sup>*EURATOM-CCFE Fusion Association, Culham Science Centre, OX14 3DB, Abingdon, OXON, UK*

<sup>2</sup>*MPI für Plasmaphysik, EURATOM Association, Boltzmannstrasse 2, 85748 Garching, Germany*

*\* See annex of F. Romanelli et al, "Overview of JET Results",  
(23rd IAEA Fusion Energy Conference, Daejeon, Republic of Korea (2010)).*

Preprint of Paper to be submitted for publication in Proceedings of the  
20th International Conference on Plasma Surface Interactions , Eurogress, Aachen, Germany  
21st May 2012 - 25th May 2012



## **ABSTRACT**

This paper reviews the transition to all metal plasma facing components from an all carbon wall in JET and ASDEX-Upgrade. This is an essential step on the path to reactor scale fusion devices and has been a major focus of work in tokamaks and laboratory based experiments in recent years. The transformation of ASDEX-Upgrade to an all tungsten (DEMO-like) wall, and recent installation of the ITER-like Wall (ILW) in JET, allows direct comparison of operation with all carbon plasma facing components (PFCs) to all metal walls under otherwise nearly identical conditions. There has also been a unique opportunity to compare and contrast operation with a beryllium wall and tungsten divertor in JET with an all tungsten PFCs in ASDEX-Upgrade. The scope of this review ranges from experience with machine conditioning, impurities and breakdown to material migration, fuel retention, disruptions, impact on operational space, energy confinement and compatibility with impurity seeding. Significant changes are reported, not only in physics directly related to plasma-surface interactions but also to the main plasma which is strongly affected in unexpected ways, impacting many aspects of tokamak operation.

## **1. INTRODUCTION**

This paper provides a review of the impact of the new JET ITER-like wall (JET-ILW) [1], with its beryllium main wall and tungsten divertor, on plasma-surface interactions and plasma operations with reference to the carbon wall phase of JET (JET-C) [2]. Parallels are also drawn with existing experience on ASDEX-Upgrade which changed from all carbon (AUG-C) to all tungsten (AUG-W) plasma facing components (PFCs) [5]. A beryllium main wall and tungsten divertor were selected for the DT phase of ITER because of the high tritium retention associated with carbon co-deposition [3] and the operational flexibility anticipated for a low Z main wall. A full tungsten wall is however considered more relevant for DEMO [4] and has been the focus of studies with an all tungsten wall in ASDEX-Upgrade (AUG-W) in recent years [5], [6]. The transition in ASDEX-Upgrade from full carbon (AUG-C) to full tungsten walls provides valuable parallels for comparison with JET and will be used as the primary reference. We do not claim that similar results may not been reported in other tokamaks or laboratory experiments but these two machines offer a particularly clean comparison of all metal with all carbon walls with other factors kept essentially constant and ITER relevant plasma configurations. An invited review of ASDEX-Upgrade operation with tungsten walls is also provided by Neu in the same conference proceedings as this paper and should be seen as the companion paper where the ASDEX-Upgrade related detail and references can be found [5].

## **2. RESIDUAL IMPURITY LEVELS**

JET has a long history of experiments with beryllium limiters, beryllium divertor tiles and the use of beryllium evaporation [54] but large areas of carbon remained and tended to dominate due to the effect of chemical sputtering [8] and transport to remote areas [9], [10]. The ITER-like wall was installed in a single shutdown with all but a few special tiles installed by remote handling. No cleaning of the naked vessel or support structures, other than vacuuming to remove residual carbon

particles, was undertaken. In contrast, ASDEX-Upgrade had a gradual change to full tungsten over a number of years but despite careful cleaning the carbon concentrations only fell from 2-3% down to 0.8-1.8% until boronisation [11]. After boronisation the carbon levels temporarily fall by one order of magnitude, recovering to the pre-boronisation levels after about 100 pulses. Several such boronisations are typically carried out each year.

After installation of the JET ITER-like Wall (JET-ILW) the vessel was baked to 325°C, glow discharge cleaning in deuterium was carried out for about 100 hours and the temperature reduced to 200°C for first plasma [12]. There had been considerable debate on the need to clean the JET vessel of residual carbon after the CFC tiles were removed but in the end it was considered too costly in time and probably not needed. This proved a good decision because in the first phase of JET operation with the ITER-like Wall, the CIII (97.7nm) line intensities measured in the main chamber were reduced with respect to the carbon wall (JET-C) by a factor 20 on average [13], Fig. 1. A similar decrease was seen in the CII(426.7nm) emission from the outer divertor and carbon concentrations derived from charge exchange resonance spectroscopy also show a similar reduction. Oxygen levels with the JET-ILW were one order of magnitude lower than at the start of the carbon wall reference campaign (JET-C). However, in the JET-C campaigns conditioning and beryllium evaporation onto the carbon wall eventually reduced the oxygen level temporarily down to that seen at the start of JET-ILW. After first diverted JET-ILW discharge was established a series of repeat discharges was carried out to study the evolution of residual impurities and migration of Be and W prior to significant mixing [7]. This represented a unique opportunity to study material migration from a well defined starting condition. The timescales for each impurity species to reach equilibrium varied and depended on the area under observations but typically after ~100 identical pulses the system approached equilibrium [7].

The lower residual carbon level observed in JET-ILW compared to AUG-W is thought to be mainly due to gettering of carbon and oxygen by beryllium. Beryllium gettering is intrinsic to plasma operation due the relatively high sputtering yield of beryllium, combined with an ability to form a stable oxide. Boronisation plays an equivalent role with the W wall in ASDEX-Upgrade but boronisations are infrequent and the effect on residual carbon is relatively short lived. Carbon levels seen in AUG-W are only comparable to those typical of JET-ILW just after boronisation.

## ***2.1 PLASMA BREAKDOWN AND WALL CONDITIONING***

With the carbon wall in JET, establishing first plasma following venting of the vessel has always required a number of attempts. Multiple conditioning cycles based on low discharge cleaning (GDC) in deuterium and beryllium evaporation were required and first breakdowns were not sustained for very long. In contrast, the first plasma with ITER-like Wall reached a plasma current of 1MA at the first attempt and lasted 15s - totally unheard of with the carbon wall. Since then, there have been no failed breakdowns attributable to conditioning issues and no need for GDC or beryllium evaporation despite the presence of a significant air leak. In Fig 2, the radiated power at the end of the burn-through phase is compared between JET-ILW and JET-C and shows the lower radiation and

higher density with the beryllium wall [14]. This behaviour has been reproduced for the first time by modelling the breakdown including plasma-surface interactions effects [15]. Carbon radiation at burn-through fell by an order of magnitude as the ILW campaign proceeded, hence the vertical range of the data. Disruptions with JET-ILW also have no effect at all on the subsequent breakdown in contrast to the carbon wall where failed breakdowns occurred in 27% of subsequent discharges [14].

A similar comparison of the effect of PFC material on breakdown cannot be made between AUG-W and AUG-C due to other system changes over the years of the wall changeover. After completion of the full tungsten wall in ASDEX-Upgrade, helium GDC was initially used as frequently as for the carbon wall (~2 min after each discharge). This was subsequently changed to a 2 min deuterium glow typically once a day. In both AUG-W and JET-ILW, improvements in breakdown and conditioning are related to reduced retention of fuel and gaseous impurity species by the all metal wall leading to better control of initial density and lower radiation. In both machines, seeded impurities such as nitrogen and argon are also released at a sufficiently low level that they usually do not impact subsequent breakdowns [16,17]. Retention of He in AUG-W and release in subsequent plasmas was a problem for confinement which is why the conditioning method was changed [5] but there is no equivalent experience yet with JET-ILW. With the carbon walls, more obvious legacy issues for gaseous impurities were observed in both tokamaks.

### 3. FUEL RETENTION

The most persuasive justification for the selection of a tungsten divertor and beryllium wall for the DT phase of ITER has been a requirement to keep long term tritium retention low enough to comply with safety limits. Predicting the tritium retention in ITER is a complex problem with many uncertainties. Most often cited is a paper [3] which predicts a factor ~10-50× reduction in fuel retention in ITER for a beryllium wall and tungsten divertor as compared to a full carbon wall. This analysis is based on laboratory data combined with assumptions about the plasma-wall interactions in ITER. In the same reference, a full tungsten wall is predicted to reduce tritium retention by a factor ~20-100× with respect to an all carbon ITER.

Fuel retention rates from gas balance studies for JET-ILW are compared with JET-C in Fig. 3 [18], where the retention rate is calculated with respect to the time spent in the divertor configuration. Gas consumption for JET-ILW is actually higher in the limiter phase compared to JET-C but lower in the divertor phase with higher outgasing after the pulse [19] leading to the lower overall retention. The ratio between JET-ILW and JET-C results is 10-20× for matched scenarios, Fig. 10. Because the fuel retention is much lower with the ITER-like wall, errors in the gas balance have become more significant. Some gas balances were therefore carried out without divertor cryo-pumping, Fig.3, which significantly reduces the gas throughput and increases the accuracy. The results are similar which gives confidence in the method.

ITER needs a retention rate  $< 10^{20} \text{ s}^{-1}$  for tritium [3] when running 50:50 DT plasmas. The JET retention data in Fig. 3 should be divided by 2 for comparison with the ITER number because we have been using pure D plasmas so far. The absolute retention rate for JET-ILW therefore lies just

below the ITER requirement but without any scaling factor applied. The same models used for the ITER predictions have not yet been applied to JET-ILW. This means that while the relative retention between JET-C and JET-ILW is encouraging, we can not yet say that the absolute level is consistent with ITER modelling assumptions.

It is important to note that gas balance analysis which is carried out over one operational day only gives an upper limit on the long term fuel retention. Experience from the JET tritium campaign showed that long term retention with a carbon wall is significantly lower than that derived from gas balance measurements [20]. This was assumed to be due to outgasing over longer periods of time and the outgasing behaviour of JET-ILW between pulses suggests that the same may be true now [19]. JET is scheduled to remove the first ILW tiles for surface analysis in autumn 2012 after 2 weeks of repeated H-mode discharges and the results will be essential for determining a lower limit for the fuel retention.

ASDEX-Upgrade has carried out gas balances and surface analysis in both the carbon and all tungsten phases [21]. The fuel retention rate with the full tungsten wall was only 5-10× lower than for the carbon wall as determined by surface analysis [22] (long term retention is at the noise level for the gas balance). Long term fuel retention rates were therefore reduced by less than the factor 20-100× predicted in the context of ITER[3]. A closer examination of the data reveals that the fuel retention in AUG-W is almost entirely attributable to co-deposition with residual carbon [22]. Higher retention in the tungsten also results from the room temperature walls but taking this into account, the levels attributable to the tungsten are consistent with the models used for ITER [5]. Although residual carbon (and boron) levels are much lower in JET-ILW than AUG-W, until surface analysis results are available from JET-ILW we will not be able to tell if it makes a significant contribution to the long term retention rate or determine the lower limit of the fuel retention.

In summary, we expect that co-deposition with beryllium will be the primary source of long term retention in JET-ILW with a lesser contribution from residual carbon. In AUG-W the residual carbon is known to dominate over retention in the tungsten coated PFCs.

#### **4. PRIMARY IMPURITIES FROM PFCs**

The original choice of an all tungsten divertor for the ITER-like Wall was made to provide a clean result in the absence of carbon. Since then, ITER has selected a full tungsten divertor for its DT phase and there is currently a strong interest in proving its suitability as a first divertor for ITER [23]. High Z materials have the potential to severely restrict the operational space of a tokamak [4] and melting [24] is an additional risk not present with carbon. Beryllium on the other hand has a high and still uncertain erosion rate with the potential for short component lifetimes and high tritium retention [3].

##### **4.1 TUNGSTEN SPUTTERING**

Spectral lines associated with neutral tungsten are visible in both the outer and inner divertor of JET-ILW and as in AUG-W are being used to evaluate the sputtering yields and general behaviour of the sources. Results from the two machines are very similar with sputtering by low Z impurities

dominating under normal circumstances [25], [56]. This is due to the high threshold energy for sputtering of tungsten by deuterium. In both machines, the sources decrease strongly with density and increase with input power as expected given the link between divertor temperature and ion impact energies. These observations are an old story seen in a wide range of devices. The effective tungsten sputtering yields are plotted in Fig.4 as a function of divertor electron temperature for both AUG-W and JET-ILW [25]. In both cases, low Z impurities are required to explain the yields. Sputtering yields in JET-ILW are much lower because beryllium ions are lighter than their carbon counterparts which dominate in AUG-W. Another important difference is that the absolute concentration of Be is lower in JET-ILW than C in AUG-W. This is particularly the case at low electron temperatures because the beryllium physical sputtering decreases strongly whereas carbon chemical erosion which is significant in AUG-W does not.

Another similarity between the JET-ILW and AUG-W is the effect of seeded impurities [26], [27], [25], [55] which at low dosing levels can increase the W source but at higher levels the cooling effect takes over and the net source decreases in both L and H-mode (inter-ELM). As previously seen in AUG-W [28], ELM heat pulses in JET-ILW increase the sputtering rate [25]. This is true even at high densities where the inter-ELM sources are low.

#### **4.2 TUNGSTEN ACCUMULATION AND PEAKING**

Although a quantitative comparison of AUG-W with JET-ILW is not possible yet because the analysis of the JET data is ongoing, the two machines show very similar behaviour [29] with respect to tungsten accumulation and peaking. In H-mode, low ELM frequency (typically less than 10Hz) often leads to W peaking, a high core radiation level and ultimately to collapse of the central temperature and hollow profiles, Fig. 5. If the sawtooth instability is not maintained inside the  $q=1$  surface, then W peaking is also more likely (note decay of sawtooth activity in Fig. 5).

In ASDEX-Upgrade, central heating by ECRH is routinely used to prevent W-peaking [5]. In JET, sufficient central heating can be obtained under some conditions by optimising the neutral beam power deposition. In JET, on-axis ICRH has also been used successfully to control W-peaking during the current ramp-up phase. In both machines, gas fuelling reduces the tungsten influx and helps to produce sufficient ELM frequency to purge the tungsten from the main plasma. Given the right balance between these factors an acceptable and stable W concentration can be achieved.

#### **4.3 MEDIUM TO HIGH Z PARTICLE INFLUXES**

Spikes in total radiated power are often seen with JET-ILW but are more frequent when there is a change in plasma shape. These events are thought to be due to small particles of medium or high Z material entering the plasma. Fig. 6 shows an analysis of the frequency and composition of such particles based on core spectroscopy from the first 1300 pulses with JET-ILW. About 65% of the particles were identified as being composed of tungsten, 24% were nickel and 8% iron. An analysis of the same event data set for magnitude of radiation spike shows a peak at 25% of total input power but with a long tail so that about 70% of events cause a perturbation of less than 60%. An H-mode discharge is more likely to recover from such events if the ELM frequency is high and there is strong

sawtooth activity in the core. The effective size of tungsten particle implied by the typical radiation spike and spectroscopic measurements of the total tungsten content of the plasma is of the order of 0.1mm. This is a lower limit for the particle size because there may be losses near the edge of the plasma where the impurity confinement time is short. In the next planned intervention, the dust will be collected for characterisation and this will allow a quantification of the screening factors. The nickel particles seen in JET may originate from remote cutting of some Inconel (~58%Ni, 21%Cr, 9%Mo) brackets which carried out during the ILW installation.

A similar analysis of radiation events has not been carried out for AUG-W and this is because they are less obvious or less frequent than for JET-ILW. There are a number of possible reasons for this: particles can be seen in IR images sitting on the horizontal surfaces of the JET divertor and there is clear evidence that more events are seen when such areas are accessed by the plasma. The AUG divertor has much less horizontal surface area and so may not accumulate particles in areas accessible to the plasma. In addition, there may be fewer particles. This is because although the divertor tungsten coating process used is the same as that developed for JET-ILW, the substrate is fine grained graphite (FGG) rather than 2D carbon fibre composite CFC. FGG is smoother and has a better thermal expansion match to the coating making small delaminations less probable [30]. Better screening by the AUG-W divertor is another possible difference because the divertor in AUG has similar geometric size and tends to operated at higher density. The number of W radiation events has decreased with time as the NBI power has increased which suggests that thermal fatigue of the W-coatings is not the primary source. The total area of exposed carbon implied by the number of particles is miniscule and there has been no significant rise in residual carbon levels [13].

#### ***4.4 EFFECT OF HEATING METHOD ON SOURCES***

Installation of an all tungsten wall in ASDEX-Upgrade created a problem with ICRH heating which had not been seen with the carbon wall [28, 31]. Total radiated power increased strongly with ICRH almost equalling the input power due to a rise in tungsten concentration. The primary source of the tungsten influx was identified as the ICRH limiters surrounding the antenna rather than the divertor. It was therefore expected that the situation with the JET-ILW would be very different since the antenna surrounds and all components closest to the plasma are made of solid beryllium. Experiments were carried out with JET-ILW directly comparing the response of a constant density L-mode plasma to equal amounts of neutral beam (NBI) and ICRH heating, Fig.7. This showed that the power radiated from inside the separatrix (bulk radiation) is much greater with ICRH [32], particularly at low plasma density. Despite this high power loss, it is interesting that the rise in plasma stored energy (not shown) is very similar in the two heating phases. As one might expect, most of the radiated power ( $\geq 70\%$ ) can be attributed to tungsten, an analysis based on the continuum radiation measured with VUV spectroscopy [33] is shown. Estimates of the contribution of Ni to the radiation from the main plasma during ICRH suggests that it may be the second most important at around 30%. What is surprising is that the outer divertor tungsten source at the bulk W tile where the strike point is located appears to be 40% lower during the ICRH

phase. Studies of the outer divertor baffle area show no substantial rise either. There are tungsten coated tiles in recessed areas of the main chamber of JET-ILW but as yet there is no definite link established to these yet either although a significant W level is still seen in ICRH heated limiter discharges. The cause of the increased radiation during ICRH in JET-ILW remains the subject of ongoing investigation and analysis [32].

#### **4.5 BERYLLIUM**

Determination of the sputtering yield and sources of beryllium remains a critical issue for ITER due to a wide variation in published data between tokamaks and laboratory experiments [3]. Erosion yields have now been studied in well diagnosed limiter plasmas with the JET-ILW but extracting the yields still needs detailed modelling [34]. In Fig.8,  $Z_{\text{eff}}$  measured in inner wall limiter discharges over a wide range of density is shown. The plasmas are very clean at high density whilst at low density self sputtering causes a rapid rise in beryllium content up to the theoretical limit where  $Z_{\text{eff}}=4$  which corresponds to a fully ionised beryllium plasma. Diverted H-mode plasmas in JET-ILW typically have  $Z_{\text{eff}}$  in the range 1.2-1.4, which should be compared with the typical range in JET-C of 1.8-2.5 [35].

At the start of operation with JET-ILW beryllium levels in the outer divertor increased and finally stabilised after the first ~800 discharges showing an inverse relationship to the residual carbon which suggests gettering by the beryllium [13,7]. Information on the distribution and amount of beryllium deposition must await removal of the long term samples later in 2012. A positive result for heat flux measurements is that while with JET-C, Be/C layers made IR thermography more difficult due to their thermal resistance, an equivalent effect is not seen with JET-ILW [36].

### **5. DISRUPTIONS**

Disruptions are a critical issue for ITER because of the high thermal and magnetic energies that are released on short time scales, resulting in extreme forces and heat loads. The most important difference between JET-ILW and JET-C is the absence of strongly radiating impurities during the disruption process [17]. This has significant implications: a) low radiation during the current quench phase, b) a hot current quench plasma, c) long current decay times (often limited by vertical displacement), d) high heat loads caused by conduction of magnetic energy to PFC, e) higher halo current fractions disruptions without vertical displacement events (VDEs). Because of these consequences, massive gas injection (MGI) with Ar/D<sub>2</sub> mixtures is now an important tool in JET for preventing the increased mechanical loads and extreme heat loads which have led to localised melting of beryllium upper dump plate tiles. MGI has also been used routinely in AUG-W [37] above 0.9MA. Although there has been no published comparison between disruptions in AUG-W and AUG-C, the JET-ILW results have led to an examination of the relevant data and many similar features are apparent [38].

In JET, the fraction of radiated energy has dropped from 50-100% of the total magnetic and

thermal energy dissipated in the plasma with the carbon wall to <50% and down to 10% for a vertical displacement event (VDE). These numbers exclude the magnetic energy which couples into circuits outside the vessel. The lack of radiation results in high plasma temperatures after the thermal quench with  $T_e$  up to 1 keV being observed. Due to the resulting low resistance, the current decay is extremely slow. With the carbon wall about 80% of all unmitigated disruptions had a linear current quench time below  $6\text{ms/m}^2$ , whereas with the JET-ILW only 15% are that fast and 20% have a very long current quench well above  $20\text{ms/m}^2$ . The slow current quench times facilitate vertical displacement during the current quench and a high halo current fraction is more likely.

The heat fluxes to first wall components have dramatically increased with the ILW, because of the low radiation. Temperatures close to the melting limit have been locally observed on upper first wall Be structures during deliberate VDE and even at plasma currents as low as 1.5 MA and thermal energy of about 1.5 MJ. Local melting has been detected on the exposed ends of these secondary protection structures by regular video inspection. A high radiation fraction can be regained by massive injection of a mixture of 10%Ar with 90%D2. MGI accelerates the current quench and thus reduces the halo current fraction below 10%, the vertical vessel forces by up to 50% and the sideways forces virtually to zero. Because of the high radiation, the temperature of the Be stays below 400°C. Non-sustained breakdowns in the pulses following the injection of D<sub>2</sub> mixtures as observed with the C-wall are absent with the ILW. If disruption avoidance fails, MGI is essential for machine protection. It has been successfully applied in JET to mitigate disruptions by triggering on mode lock amplitude.

The lack of carbon radiation in JET-ILW has also raised the disruptive density limit in L-mode [39], [40] by 40% in the ITER relevant vertical target configuration. At the same time there is much wider stable detachment window in the outer divertor. Roll over of the ion flux occurs at the same radiated power fraction showing that the detachment process does not directly involve carbon related physics [40]. In the transition from AUG-C to AUG-W there was no significant change in density limit presumably due to the relatively high residual carbon.

## **6. POWER HANDLING**

Considerable effort went into design, quality control and careful installation of the JET-ILW to ensure that the tile profiles were optimised to maximise the power handling and that no edges above 40µm effective height were exposed in high heat flux areas [41], [42]. In addition, an integrated protection system for ITER-like Wall (PIW) was implemented which uses CCD cameras operating in the near infra-red to trigger context determined stops [43]. Experiments carried out to verify the power handling limits set by the bulk W divertor with its lamella structure [44] and wall geometry have shown that the design process has delivered the expected performance. At the time of the PSI conference there had been no melt damage to the main JET limiters and no unexpected hot spots on the inner and outer wall limiter surfaces. The only exception to this was a single small melt spot near the bottom of one inner wall guard limiter. This was caused by a runaway electron beam created by an emergency stop procedure (now modified) which worked well with the carbon wall

but did not account for density pump-out by the beryllium wall in the limiter phase.

AUG-W has used a similar set of filtered CCDs to the JET system to provide protection for the W-coatings used in the divertor and much of the main wall by limiting temperatures to  $<1200^{\circ}\text{C}$  [45]. In JET-ILW, real-time algorithms had to be developed to avoid false triggering by mobile hot particles which are frequently seen sitting on horizontal divertor surfaces which has not been a problem for the vertical target in AUG.

## **7. SCENARIOS**

We expected that changing the wall from all carbon to all metal in JET would have little impact on the phenomenology and physics of scenarios other than impose new constraints on operating space in order to control tungsten accumulation and avoid melting of beryllium tiles. In reality, the landscape of the edge operational space has significantly changed for JET-ILW and looking at AUG-W data we see many similar features.

### **7.1 L-H POWER THRESHOLD**

Changes in core radiation with the transition to ILW might be expected to shift the L-H threshold expressed in terms of total input power but leave it the same with respect to power crossing the separatrix ( $P_{\text{sep}}$ ). In practice, the L-H power threshold dropped by 30% at higher densities even when referenced to  $P_{\text{sep}}$  [46]. This experience is very similar to that in AUG-W where a  $\sim 25\%$  reduction is reported [5].

### **7.2 ACCESS TO HIGH ENERGY CONFINEMENT**

A low L-H threshold seems a positive indicator for obtained good confinement ( $H\sim 1$ ) at modest input power but this has been hard to realise with the JET-ILW due to the need to operate at higher gas fuelling than with the carbon wall to reduce the W sources and avoid accumulation. The ELM type boundaries have also shifted as discussed in section 7.3, meaning that type I ELMs can be observed at much lower edge temperature than in JET-C where there would have been a transition to type III ELMs. The low edge electron temperatures are associated with low H-factors. This fits the trend of decreasing H-factor with increasing gas-fuelling seen in low triangularity H-modes with JET-C. The importance of the high triangularity H-modes run on the carbon wall was that they also tolerated a somewhat higher fuelling rate allowing access to good energy confinement at higher density than for low shape scenarios[47].

Despite the constraints, JET-ILW pulses with  $H_{98}\sim 1$  have been obtained in low and high shape inductive scenarios up to 2.5MA and are associated with low fuelling rates ( $<10^{22}\text{e/s}$ ) and optimised pumping. Access is hindered by tungsten accumulation which is also associated with these conditions since they lead to high edge temperatures. In AUG-W access to good energy confinement regimes was facilitated by use of higher input powers (which increases  $f_{\text{ELM}}$ ), ELM pacing and use of central heating to control W accumulation [5,6]. A similar integration of techniques for controlling the tungsten content is ongoing for JET scenarios. These techniques aim at increasing the edge temperature whilst maintaining an acceptable W concentration in the main plasma.

The hybrid plasma scenario aims to have part of the current driven non-inductively by the bootstrap current and offers the prospect of extended pulse length and  $H_{98}>1$  allowing operation at lower plasma current. Development of this scenario in JET-ILW has only just begun but initial results are very promising. The pulse shown in Fig.9 has  $H_{98}\sim 1.2$  and  $\beta_N\sim 2.8$  which is within the typical scatter of results with the carbon wall [48] (best pulses had  $H_{98}\sim 1.4$  [49]). Further optimisation of the hybrid scenario with the JET-ILW is planned. With sufficient heating / ELM frequency, low radiated power can be maintained as seen in the example of Fig.9. Selection of neutral beam sources to optimise the central heating may also have helped maintain a low central W concentration. So far hybrid plasmas have exploited attached plasmas with low radiated power fraction but this will need to change if the scenario is to be extended to significantly higher power and longer pulse length.

### **7.3 HIGH TRIANGULARITY INDUCTIVE SCENARIO AND NITROGEN SEEDING**

The JET-C high shape scenarios are a model for the ITER inductive baseline exhibiting good energy confinement close to the Greenwald density [47]. With the JET-ILW using deuterium fuelling alone we have so far not been able to reproduce this behaviour. A well matched pair of pulses which illustrate this are 82539(ILW) and 73342(C) which had almost the same high triangularity shape (2.5MA/2.7T), very similar neutral beam heating (14MW) and deuterium gas fuelling rate ( $\sim 2\times 10^{22}$ D/s). The total radiated power and density were 40% lower with ILW, the main plasma radiation was the same as was the inter-ELM outer divertor  $D_\alpha$ . The plasma is cleaner with JET-ILW with  $Z_{\text{eff}}=1.2$  compared to 1.8 for the carbon wall reference. The diamagnetic energy for the C-wall pulse reached 6.5MJ ( $H_{98y}\sim 1$ ) while for the ILW pulse it was 4MJ ( $H_{98y}\sim 0.75$ ). This difference is related to the lower pedestal temperatures seen in fuelled high shape plasmas with JET-ILW compared to JET-C, Fig.10.

In the JET-C phase the use of nitrogen seeding was associated with a loss of energy confinement [50]. With JET-ILW however, nitrogen seeding raises the pedestal density and temperature, Fig. 10, leading to stored energies and H-factors only a bit below their deuterium fuelled counterparts from JET-C and a very good match to the nitrogen seeded pulses at similar nitrogen fuelling rates. The best  $N_2$  seeding pulse with JET-ILW gives  $H_{98}\sim 0.92$  and  $n/n_{\text{Greenwald}}=1.0$  with  $Z_{\text{eff}} = 1.5$ . Nitrogen seeding cools the edge plasma and reduces inter-ELM W sources allowing access to lower ELM frequencies and fractional radiated powers up to 60% of input, there is however still an issue with W accumulation which still needs to be resolved [51].

In AUG-W a positive correlation between H-factor and  $Z_{\text{eff}}$  has been reported [52] as with JET this is opposite to the carbon wall response to seeding (a degradation in confinement). Although the nitrogen seeded pulses in JET-ILW show a strong correlation between nitrogen fuelling rate and stored energy and achieve similar radiated power fractions to their deuterium fuelled C-wall counter parts, a clear dependence with  $Z_{\text{eff}}$  has not yet been demonstrated. The results do however strongly suggest that the carbon impurities played a role in the performance of the high shape plasma scenarios in the JET-C phase.

In JET-ILW, the type I ELMs seen in deuterium fuelled shots with low pedestal temperatures exhibit a very slow crash of the edge electron temperature which has not been reported before. This

is shown in Fig. 10a, for a deuterium pulse taken from the high triangularity data set of Fig.10. Infra-red data shows that slow crashes in pedestal temperature measured by ECE corresponds to a slow rise in divertor power and hence much reduced peak temperatures for a given change in stored energy. These benign type I ELMs exist in an edge parameter space which is below the type I/type III ELM boundary for the carbon wall, Fig 10. Also seen in Fig.11a is that after the initial 2ms temperature decay there are two classes of ELM, in one type the edge temperature recovers and in the other the decline continues at a lower rate for much longer. Raising the pedestal temperature by nitrogen seeding, as in Fig. 11b, speeds up the ELM crash and makes it more akin to that seen with the carbon wall [53]. More generally however, there are changes in ELM dynamics, even at high pedestal temperatures, following the transition to JET-ILW which are the subject of ongoing study. ELM data from AUG-W is now also being re-examined and the first indications are that there are many similarities.

## CONCLUSIONS

The ITER-like wall in JET has provided a clean comparison of an all carbon machine with the all metal environment that is most relevant to ITER. In ASDEX-Upgrade, the transition to an all tungsten wall was phased over a long period of time during which other changes were made but there are still very many similarities in the results. JET's findings have also stimulated a revisiting of old ASDEX-Upgrade data and revealed more parallels between the two.

The primary motivation for JET-ILW was the study of plasma-wall interactions in support of ITER. In this regard, the first results are very encouraging. We have found low residual carbon levels, no failed breakdowns attributable to de-conditioning or need for conditioning and a reduction in fuel retention by about one order of magnitude. The divertor tungsten source behaves pretty much as expected and the techniques needed to prevent accumulation in H-mode are similar to those developed for AUG-W. The low plasma radiated power associated with beryllium provides significantly higher L-mode density limits for JET-ILW compared to JET-C and a wider and more stable detachment window in the outer divertor [39], [40]. Another consequence of low radiation is that disruptions with the JET-ILW are slower and more of the magnetic energy reaches the wall already causing minor melting of the upper dump plate tiles prior to routine use of massive gas injection (MGI) to mitigate disruptions. Disruption with or without MGI do not lead to non-sustained breakdowns in subsequent discharges as was the case with the carbon wall. Removal of long term samples for surface analysis is a key part of the strategy to fully evaluate the plasma-surface interaction in JET-ILW and this will take place in the second half of 2012.

Low and high triangularity scenarios with JET-ILW are restricted in operating space by the need to avoid tungsten accumulation at low fuelling rates where the confinement was highest in JET-C but despite this, H-factors around unity have been obtained. Hybrid scenario development has also made a promising start achieving high normalised beta and  $H > 1$ . However, in the high triangularity inductive scenario, despite clean plasmas with low radiated power and a low L-H threshold, access to  $H \sim 1$  at high density in deuterium fuelled plasmas has so far not been achieved. These H-modes

are characterised by low pedestal temperatures and rather benign Type I ELMs which are much slower than anything noted before and seem to exist in the pedestal  $n_e$ ,  $T_e$  space that in JET-C would have been occupied by the Type III ELM regime. As previously seen in AUG-W, seeding the JET-ILW high triangularity scenario with nitrogen increases radiative losses and restores the pedestal and energy confinement producing ELMs more like those seen with a carbon wall. This behaviour suggests that the carbon level may have been a hidden parameter in the JET-C confinement behaviour for high shape fuelled scenarios. The next step for development of JET-ILW compatible scenarios will be to integrate some of the techniques used in AUG-W to open up the operational space at lower fuelling rates by controlling W accumulation while pushing to higher plasma current.

Overall, the results from the transition from carbon to all metal walls in both JET and ASDEX-Upgrade show that a full implementation of relevant wall materials is not only important for plasma-wall interaction studies but should also be an integral part of scenario development for next step devices.

## Acknowledgements

This work, part-funded by the European Communities under the contract of Association between EURATOM/CCFE was carried out within the framework of the European Fusion Development Agreement. The views and opinions expressed herein do not necessarily reflect those of the European Commission. This work was also part-funded by the RCUK Energy Programme under grant EP/I501045.

## References

- [1]. G.F. Matthews et al., *Physica Scripta* (2011) 014001
- [2]. S. Brezinsek et al., *Journal of Nuclear Materials*. **415** (2011) 936-942
- [3]. J. Roth, et al., *Plasma Phys. Control. Fusion* **50** (2008) 103001 (20pp)
- [4]. V. Philipps, *Journal of Nuclear Materials* **415** (2011) S2-S9
- [5]. R. Neu, I2, "Overview over Plasma Operation with Full Tungsten Wall in ASDEX Upgrade", 20<sup>th</sup> International Conference on Plasma Surface Interactions in Controlled Fusion (Aachen, 2012)
- [6]. A. Kallenbach et al., *Nuclear Fusion* **51** (2011) 094012 (11pp)
- [7]. K. Krieger, O28 "Beryllium Migration and Evolution of First Wall Surface Composition in the JET ILW Configurations", 20<sup>th</sup> International Conference on Plasma Surface Interactions in Controlled Fusion (Aachen, 2012)
- [8]. G.F. Matthews, *Journal of Nuclear Materials* **337-339** (2005) 1-9
- [9]. H.G. Esser et al., *Journal of Nuclear Materials* **337-339** (2005) 84
- [10]. S. Brezinsek et al., *Journal of Nuclear Materials* **337-339** (2005) 1058
- [11]. A. Kallenbach et al., *Nuclear Fusion* **49** (2009) 045007 (10pp)
- [12]. D. Douai, P3-075, "Wall conditioning of JET with ITER-like Wall (ILW)", 20<sup>th</sup> International Conference on Plasma Surface Interactions in Controlled Fusion (Aachen, 2012)

- [13]. S. Brezinsek, P1-083, “Residual Carbon Content in the Initial ILW Experiments at JET”, 20<sup>th</sup> International Conference on Plasma Surface Interactions in Controlled Fusion (Aachen, 2012)
- [14]. P.de Vries et al., “Comparison of plasma breakdown with a Carbon and ITER-like wall “, 24th IAEA Fusion Energy Conference (FEC2012), San Diego, USA
- [15]. H.T. Kim, P1-056, “Burn-through simulations including PSI effects on JET”, 20<sup>th</sup> International Conference on Plasma Surface Interactions in Controlled Fusion (Aachen, 2012)
- [16]. M. Oberkofler et al., O27, “First Nitrogen-seeding Experiments in JET with the ITER-Like Wall”, 20<sup>th</sup> International Conference on Plasma Surface Interactions in Controlled Fusion (Aachen, 2012)
- [17]. M. Lehnen, et al., I13 “Disruption Heat Loads and their Mitigation in JET with the ITER-Like Wall”, 20<sup>th</sup> International Conference on Plasma Surface Interactions in Controlled Fusion (Aachen, 2012)
- [18]. T. Loarer, I15, “Comparison of Fuel Retention in JET between Carbon and the ITER-Like Wall”, 20<sup>th</sup> International Conference on Plasma Surface Interactions in Controlled Fusion (Aachen, 2012)
- [19]. V. Philipps et al., P3-043, “Dynamic fuel retention and release under ITER like wall conditions in JET”, 20<sup>th</sup> International Conference on Plasma Surface Interactions in Controlled Fusion (Aachen, 2012)
- [20]. J.P. Coad et al., *Physica Scripta* **2011** 014003
- [21]. V. Rhode et al., *Nuclear Fusion* **49** (2009) 085031 (9pp)
- [22]. K. Sugiyama et al., *Nuclear Fusion* **50** (2010) 035001
- [23]. R. Pitts, I04, “A full tungsten divertor for ITER: physics issues and design status”, 20<sup>th</sup> International Conference on Plasma Surface Interactions in Controlled Fusion (Aachen, 2012)
- [24]. J. Coenen et al., I1, ”Evolution of Surface Melt Damage, its Influence on Plasma Performance and Prospects of Recovery”, 20<sup>th</sup> International Conference on Plasma Surface Interactions in Controlled Fusion (Aachen, 2012)
- [25]. G. van Rooij, I3, “Tungsten Divertor Erosion in all Metal Devices: Lessons from the ITER-LikeWall of JET and the all-W ASDEX Upgrade”, 20<sup>th</sup> International Conference on Plasma Surface Interactions in Controlled Fusion (Aachen, 2012)
- [26]. A. Kallenbach et al., *2010 Plasma Physics and Controlled Fusion* **52** 055002
- [27]. L. Aho-Mantila, P1-003, “Modelling of L-mode Radiative Plasma Edge in ASDEX Upgrade and JET”, 20<sup>th</sup> International Conference on Plasma Surface Interactions in Controlled Fusion (Aachen, 2012)
- [28]. R. Dux et al., *Journal of Nuclear Materials* **363–365** (2007) 112-116
- [29]. R. Neu et al., *Nuclear Fusion* **45** (2005) 209
- [30]. R. Neu et al., *Physica Scripta* **2009** 014031
- [31]. V. Bobkov, et al., *Nuclear Fusion* **50** (2010) 035004 (11pp)
- [32]. V. Bobkov, O3, “ICRF Specific Plasma-Wall Interactions in JET with the ITER-Like Wall”,

- 20<sup>th</sup> International Conference on Plasma Surface Interactions in Controlled Fusion (Aachen, 2012)
- [33]. T. Putterich et al., 2008 Plasma Physics and Controlled Fusion **50** 085016
- [34]. D. Borodin, O29, “Measurements of Beryllium Sputtering Yields from the JET High-Field Side Poloidal Limiters in Limiter Discharges”, 20<sup>th</sup> International Conference on Plasma Surface Interactions in Controlled Fusion (Aachen, 2012)
- [35]. G.M. McCracken et al., 1999 Nuclear Fusion **39** 41
- [36]. T. Eich, I7, “Empirical Scaling of Heat Flux Widths in Tokamaks”, 20<sup>th</sup> International Conference on Plasma Surface Interactions in Controlled Fusion (Aachen, 2012)
- [37]. G. Pautasso et al., 2007 Nucl. Fusion **47** 900
- [38]. G. Pautasso (IPP Garching) private communication
- [39]. A. Huber, I21, “Impact of the ITER-Like Wall on Divertor Detachment and Density Limit in the JET tokamak”, 20<sup>th</sup> International Conference on Plasma Surface Interactions in Controlled Fusion (Aachen, 2012)
- [40]. M. Groth, et al., P1-017, “Target particle and heat loads in low-triangularity L-mode plasmas in JET with carbon and beryllium/tungsten walls”, 20<sup>th</sup> International Conference on Plasma Surface Interactions in Controlled Fusion (Aachen, 2012)
- [41]. I. Nunes et al., “Be tile power handling and main wall protection”, 24th IAEA Fusion Energy Conference (FEC2012), San Diego, USA
- [42]. V. Riccardo et al., “Design, Manufacture and Initial Operation of the beryllium components of the JET ITER-like wall”, 27<sup>th</sup> Symposium on Fusion Technology (SOFT), Liege, Belgium (2012)
- [43]. G. Arnoux et al., “A protection system for the JET ITER-like wall based on imaging diagnostics”, High Temperature Plasma Diagnostics (HTPD) 2012, Monterey, California, USA
- [44]. P. Mertens et al., “Power Handling of the Bulk Tungsten Divertor Row at JET: First measurements and comparison to the GTM thermal model”, 27<sup>th</sup> Symposium on Fusion Technology (SOFT), Liege, Belgium (2012)
- [45]. A. Herrmann et al., Fusion Engineering and Design **86** (2011) 530–534
- [46]. C. Maggi et al., “The H-mode Threshold in JET with the ITER-like Wall”, 39<sup>th</sup> European Physical Society Conference on Plasma Physics (EPS2012), Stockholm, Sweden (2012)
- [47]. G. Saibene et al., Plasma Physics and Controlled Fusion **44** (2002) 1769–1799
- [48]. E. Joffrin et al., 2005 Nuclear Fusion **45** 626
- [49]. E. Joffrin et al., “Scenario development at JET with the new ITER-like wall”, 24th IAEA Fusion Energy Conference (FEC2012), San Diego, USA
- [50]. C. Giroud et al., “Integration of a radiative divertor for heat load control into JET operational scenarios”, Nuclear Fusion in press.
- [51]. C. Giroud et al., “Nitrogen seeding for heat load control in JET ELMy H-mode plasmas and its compatibility with ILW materials”, 24th IAEA Fusion Energy Conference (FEC2012), San Diego, USA

- [52]. J. Schweinzer et al 2011 Nuclear Fusion **51** 113003
- [53]. M. Beurskens et al., Nuclear Fusion **49** (2009) 125006 (13pp)
- [54]. C.G. Lowry et al., Journal of Nuclear Materials, Volumes 196–198, 1 December 1992, Pages 735-738
- [55]. A. Kallenbach et al., Plasma Physics and Controlled Fusion, **52** (2010) 055002
- [56]. R. Dux et al., Journal of Nuclear Materials **390–391** (2009) 858–863

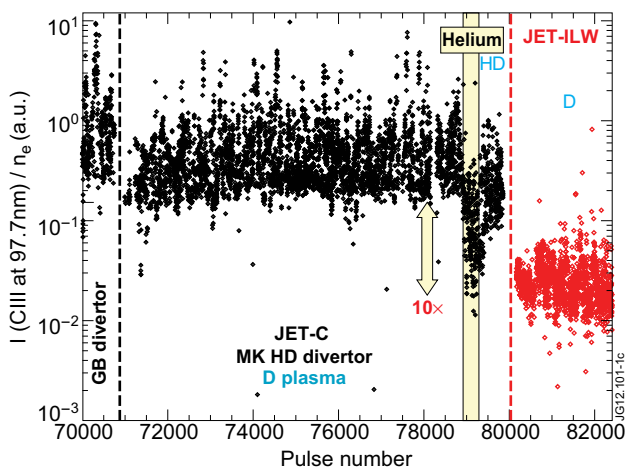


Figure 1: Intensity of CIII in the outer divertor from visible spectroscopy normalised to line integrated density at the time of X-point formation for JET-C and JET-ILW campaigns [13].

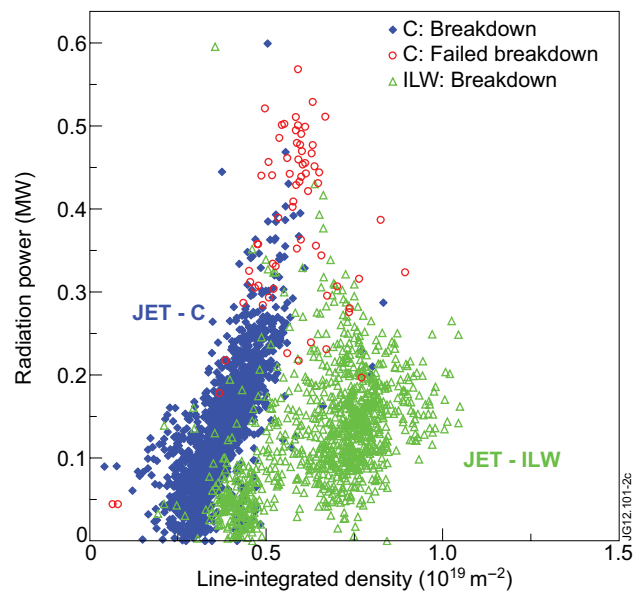


Figure 2: Radiation versus density at the end of the burn-through phase in JET [14].

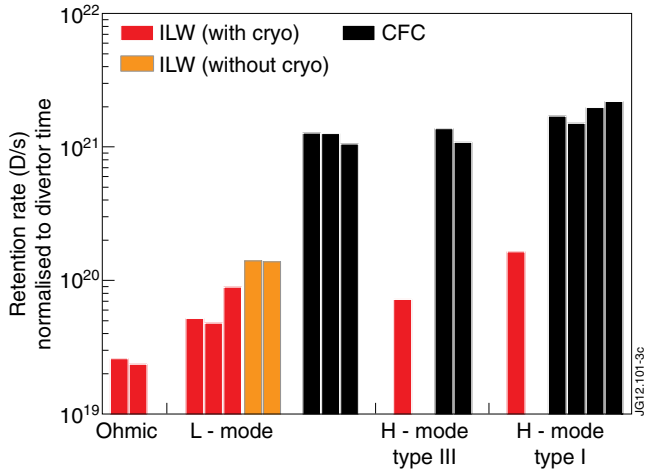


Figure 3: Fuel retention rates for JET-ILW from gas balance normalised to divertor time [18,19]. The pulses without cryo-pumping (orange) have the lowest error while the type I ELMy H-mode has the largest due to pumping by both the neutral beam and divertor cryo-pumps.

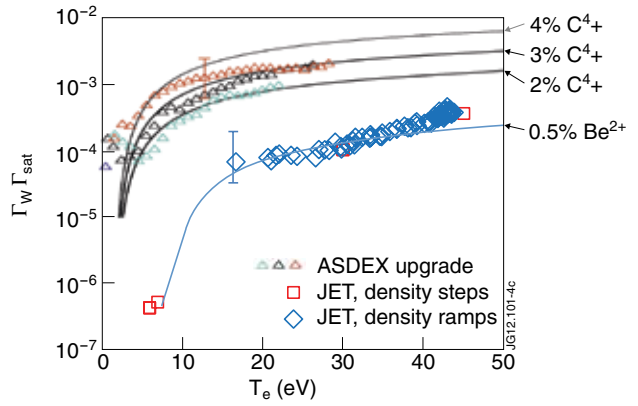


Figure 4: Effective tungsten sputtering yields for AUG-W and JET-ILW [25] vs. divertor electron temperature. Comparison is made with an analytical sputtering formula for different assumed impurity concentrations and charge states.

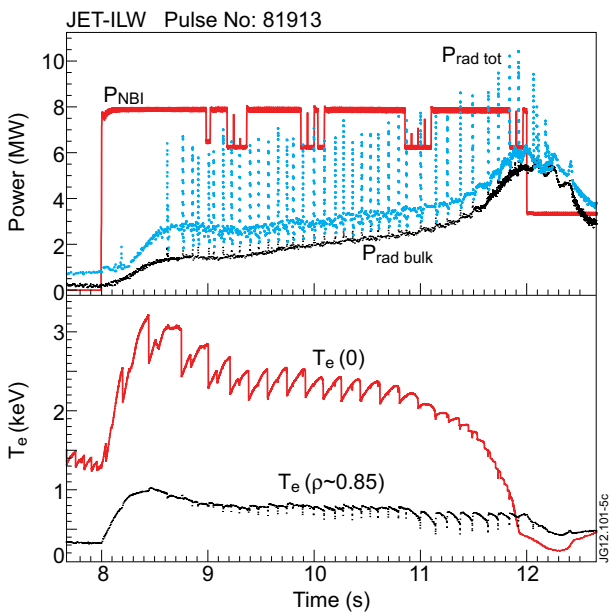


Figure 5: Extreme example of the effect of too low an ELM frequency leading to W peaking and accumulation. A rise in central radiated power leads to a collapse of the central temperature.

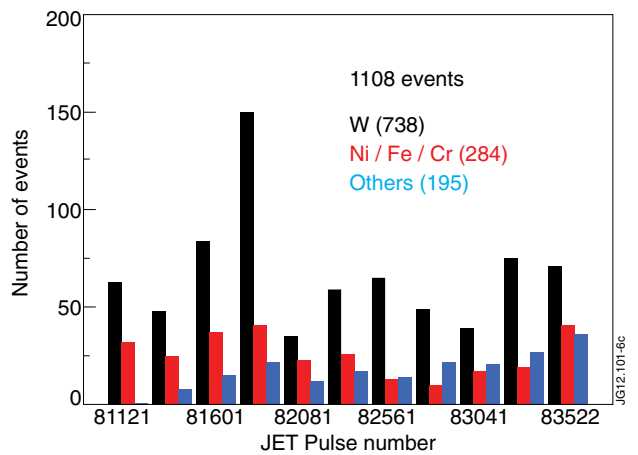


Figure 6: Frequency and composition of high Z particles detected in the first 1300 JET-ILW pulses.

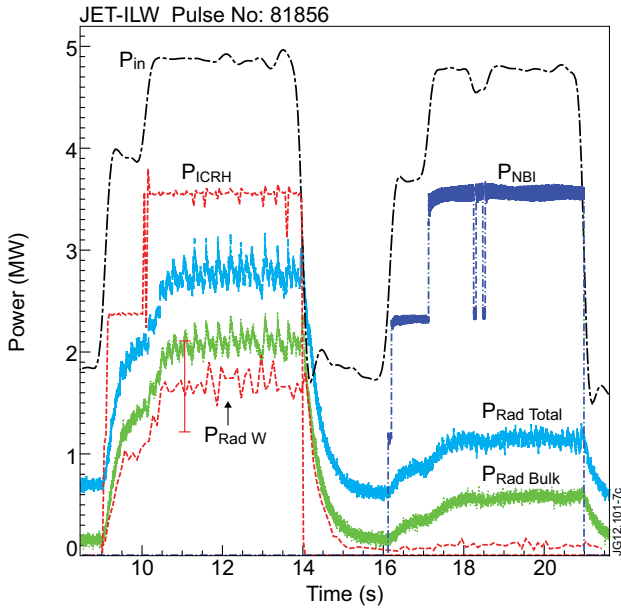


Figure 7: The effect of ICRH and neutral beam heating on plasma radiation (bolometry) is compared under otherwise constant L-mode conditions in JET-ILW pulse 81856. The radiated power from tungsten ( $P_{RadW}$ ) is calculated from continuum radiation [33].

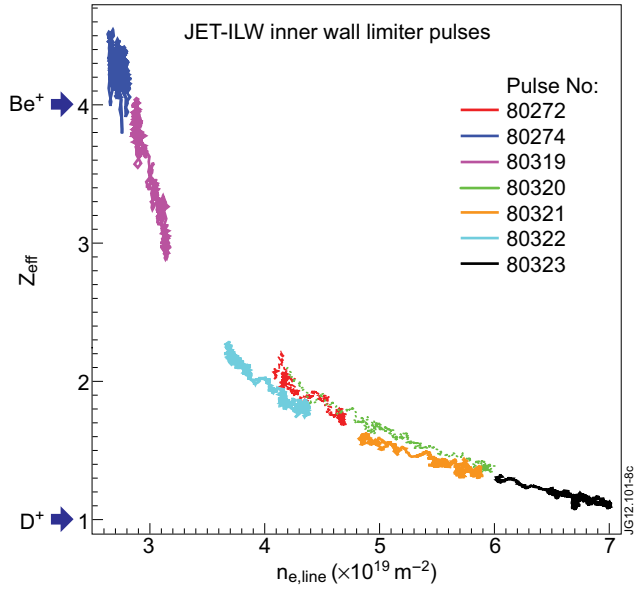


Figure 8: Line integrated  $Z_{eff}$  over a range of line integrated density for inner wall limited discharges run on JET-ILW.

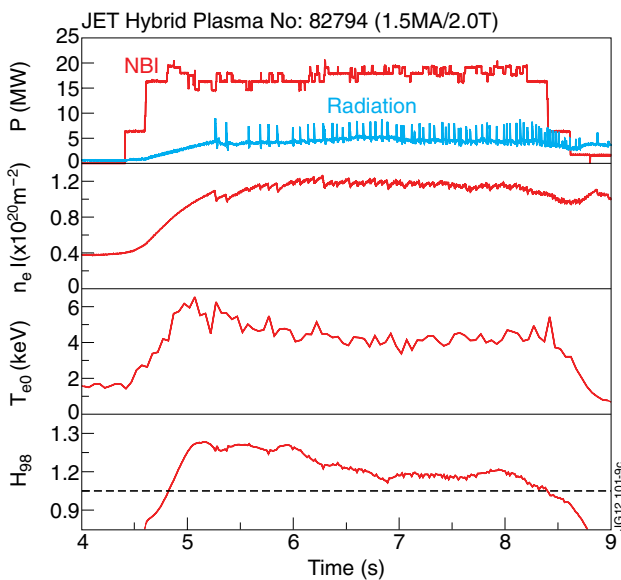


Figure 9: Pulse 82794(1.5MA/2.0T) a “hybrid” plasma [49] with JET-ILW demonstrating that  $H_{98y} > 1$  can be achieved in an optimised pulse. Note the low total radiated power and  $Z_{eff}$ .

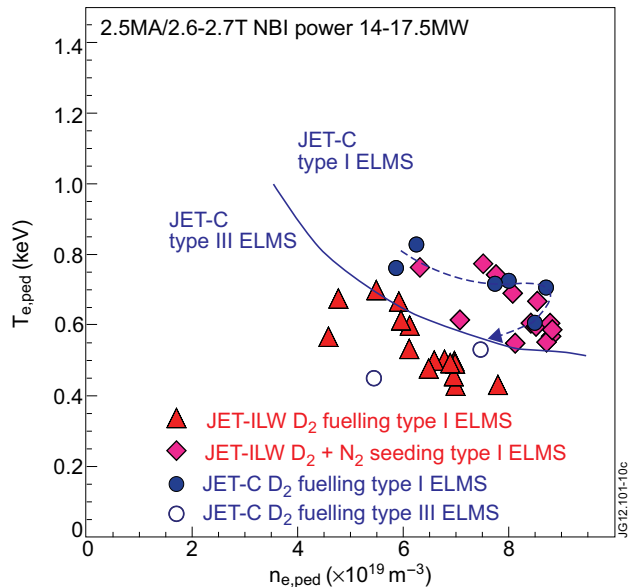


Figure 10: Pedestal  $n_e$ ,  $T_e$  diagram from Thomson scattering data for high triangularity pulses with similar input power (14-17MW) and varying deuterium and nitrogen fuelling rates for JET-C and JET-ILW. The Type I / Type III ELM boundary for JET-C is shown.

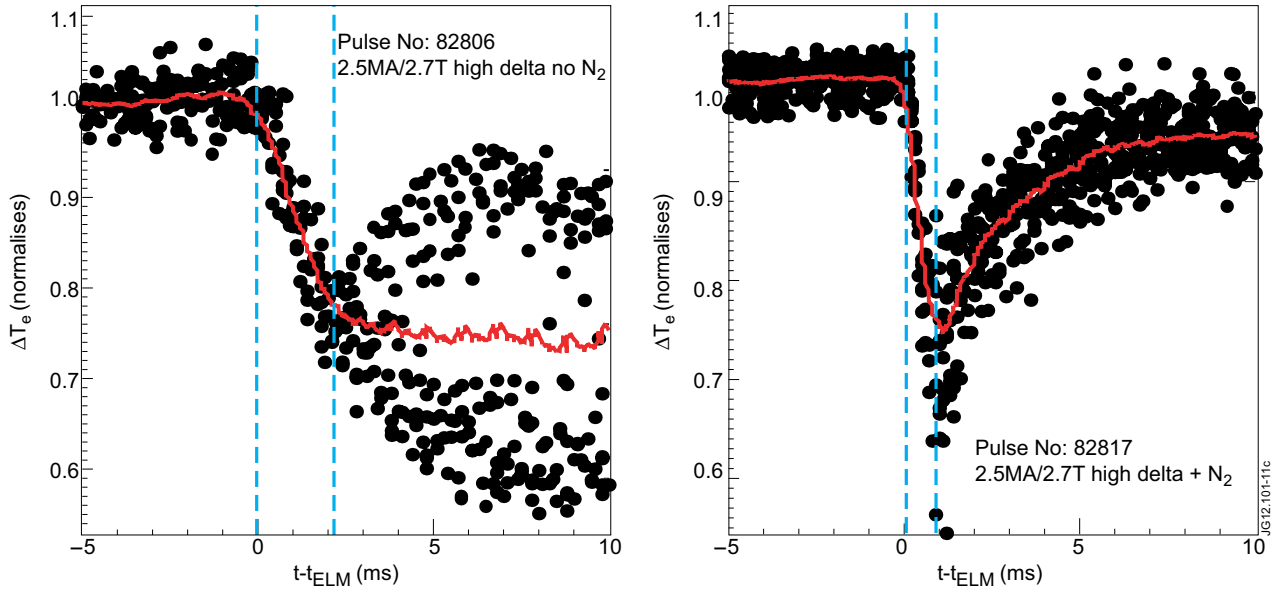


Figure 11: Edge electron temperature measured by ECE for type I ELMs (Fig.10) with JET-ILW (a) for a deuterium fuelled pulse showing a slow temperature crash ( $T_{e,ped}=500\text{eV}$ ) and a bifurcated recovery (b) a similar nitrogen seeded pulse where the crash is much faster ( $T_{e,ped}=770\text{eV}$ ).